The Focusing Optimization of Transcranial Magnetic Stimulation System

Hui Xiong[1, 2], Jin Hua Shi[1, *], Xiao Wei Hu[1, 2], and Jin Zhen Liu[1, 2]

Abstract—The transcranial magnetic stimulation (TMS) technology development becomes a painless, noninvasive, green treatment and detection method in recent years. However, because of the difference in efficiency of the stimulation system, the technology is not widely used. The focality of the magnetic field is one of the key issues that affect the efficiency of magnetic stimulation. If the focusing problem cannot be solved, the development of TMS technology will be restricted. Therefore, research of focusing has become a hot spot in recent years. In this paper, we mainly carry out three meaningful works. First, a hybrid algorithm is proposed based on a simplified particle swarm optimization algorithm (sPSO) and simulated annealing (SA) algorithm. The convergence of those algorithms is tested. The current through the coils is optimized and solved. Second, the influence of discharge circuit parameters on the magnetic field distribution in the head model is analyzed. Finally, five array coils are established, and the related parameters are configured by using the results of above research. The simulation results show that the hybrid algorithm can improve focality performance. The hybrid algorithm is made up of sPSO and SA. The proposed optimization algorithm and the study to the parameters of the discharge circuit are useful to enhance the focality of the TMS technology in the further development.

1. INTRODUCTION

Transcranial magnetic stimulation (TMS) is a non-invasive technique that has high research value and wide application prospect, including the study of normal and pathological brain function and treatment of neurological and psychiatric disorders. In 1985, Barker et al. successfully stimulated the cerebral cortex, which announced the birth of TMS [1]. From the point of clinical view, TMS may evoke some side effects. Therefore, the focality of magnetic-field distribution becomes particularly important [2]. Focality performance of the magnetic field is one of the key problems which affect the efficiency of the magnetic stimulation [3]. Thus, the study of focality is becoming a new hot research issue. The ideal curve of a focusing magnetic field distribution called "focusing curve" is similar to the spike pulse. So the magnetic field only affects the target tissues rather than the non-target tissues. However, the ideal curve cannot be achieved because of the limitation of conditions.

The conclusions are that the coil geometry and size [4], electromagnetic characteristics of human physiological tissues and coil placement direction and position [5, 6] can affect the focality. At present, the most commonly used coil in clinical medicine is "8" coil. The "8" coil has a better focality. In 2012, Yang et al. designed a double "8" coil and seven array coils in the same plane. The double-"8" coil has the same focality as the "8" coil, but the stimulus intensity is greater than the "8" coil [7]. The magnetic field distribution trend of seven array coils is similar to the circular coil, but the stimulus intensity of the former is better than the latter. Circular coil is suitable for deep brain stimulation, but the focality of the circular coil is not as good as the "8" coil [8]. In 2012, Li et al. designed a butterfly coil. Experimental results show that the focusing of a 2-disc coil is better than the butterfly coil [9].

In 2013, Zhang et al. proposed a focusing method by using a shielding plate. The shielding plate used copper with high permeability to focus the magnetic field, which can effectively enhance the focus [10]. In 2013, Gomez et al. proposed a multi-channel coil array based on genetic algorithm achieving 2.4 cm stimulus depth in the head. Compared to the traditional "8" coil, the stimulus volume decreases by 3–2.6 times [11]. In 2014, Lu and Ueno proposed a cone coil, H coil, Halo coil, and a plurality of coaxial circular coils. The cone coil and H coil can increase the depth of stimulation but decrease the focality relatively. The Halo coil and the traditional circular coil can be used together to produce the same stimulation depth with cone coil and H coil. Multiple coaxial circular coils can be more flexible to achieve the stimulus depth and focus [12].

The focusing optimization of TMS system mainly includes two aspects. The first aspect is the reasonable choice of discharge circuit parameters R, L, C. The second aspect is the parameters optimization of the coil. At present, most of the research focuses on the design and optimization of the coil structure. Laudani et al. to obtain the desired magnetic field profile (MFP), adopted the continuous flock-of-starlings optimization (CFSO) algorithm to optimize the seven and eight array coils' current intensities [13]. The research of the discharge circuit and coil placement is very little. Therefore, the optimization of coil configuration and parameters of the discharge circuit are the optimization research contents in this paper.

In the study of magnetic focusing, the structure of the coil model plays a vital role [14–16]. There are many parameters affecting the focality performance, such as electric current, number of turns, and location. As a result, the solution space is very huge, which needs a high-efficiency algorithm to find the optimum solution quickly and accurately. At present, most of the algorithms for improving the focality performance concentrate on the genetic algorithm (GA) and modified genetic algorithm. GA has good convergence and high robustness. However, GA is so complex that it cannot solve large-scale computational problems efficiently.

Although the traditional particle swarm optimization (PSO) algorithm has the advantages of quick and high quality solution in low dimensional space function optimization problems, the optimal performance decreases sharply and gets into the locally optimal solution once the dimension of the function increases. Most of the optimization of the PSO makes it more complicate [17, 18], which leads to the decline of the convergence speed and precision. As a result, a simplified, fast and accurate algorithm is needed. A simplified and efficient PSO algorithm putting forward by Wang and Li [19] can greatly improve the convergence speed and precision, which conforms to the requirement of the algorithm in this paper.

Although the modified PSO proposed by Wang and Li [19] can greatly improve the convergence speed and precision, it may get into the local optimal solution because of the lack of velocity item. Moreover, the PSO algorithm has its own flaws. At present, there are a large number of studies about improving PSO by using simulated annealing (SA) [20]. But these algorithms still have the problems of slow convergence speed and low convergence precision, especially the high-dimensional multimodal optimization complex problems such as focality optimization. This article proposes a modified method based on the modified PSO proposed by Wang an Li [19], and combines the modified PSO and SA algorithm, which can improve the calculation speed and precision.

2. THE FOCALITY PERFORMANCE OPTIMIZATION ALGORITHM

2.1. Modified Particle Swarm Optimization Algorithm

According to the simplified and efficient PSO algorithm proposed by Wang and Li [19], the particle velocity cannot represent whether the particle can be close to the optimal position or not. On the contrary, it may make the particle deviate from the correct direction and lead to slow convergence speed and low convergence precision. The final result of the optimization makes the particle position reach the optimal position infinitely. So the concept of particle velocity is not required and only the position considered. In a D dimension search space, the population is composed of m particle swarm. x_{id} is the location of the number i particle, p_{id} the individual optimal solution and p_{gd} the global optimal solution. The optimized particle swarm can be simplified as

$$x_{id}^{t+1} = \omega x_{id}^t + c_1 r_1 \left(p_{id} - x_{id}^t \right) + c_2 r_2 \left(p_{gd} - x_{id}^t \right) \tag{1}$$

where $i = 1, 2, \ldots, m$; $d = 1, 2, \ldots, D$; ω is the inertia weight; c_1 and c_2 are the learning factors; r_1 and r_2 are the uniformly distributed random number. Equation (1) is transformed to differential equation of the first order:

$$x(t + 1) + (\varphi - \omega)x(t) = \varphi\rho \tag{2}$$

where $\varphi_1 = r_1 c_1$, $\varphi_2 = r_2 c_2$, $\varphi = \varphi_1 + \varphi_2$, $\rho = \frac{\varphi_1 p_0 + \varphi_2 p_g}{\varphi_1 + \varphi_2}$.

There is no velocity item in the modified PSO equation, and the differential equation is the first order. So the analysis and evolutionary process of the modified PSO are simpler than basic PSO.

2.2. Hybrid Algorithm

Particles follow the optimal particle in the solution space. The solution updates through comparing with the optimal solution, which may lead to particle gathering and producing "premature". This is the reason that the algorithm falls into a local optimum. Simulated annealing (SA) algorithm has probabilistic jumping ability in the search process. It is capable of avoiding the local optimum. SA accepts not only the good solution, but also the bad solution at a certain probability. This probability is controlled by the temperature. The probability decreases as the temperature declines. The adaptive value of each individual extremum is determined by

$$TF(p_i) = \frac{e^{-(f(p_i) - f(p_g))/t}}{\sum\limits_{i=1}^{N} e^{-(f(p_i) - f(p_g))/t}} \tag{3}$$

An alternative global optimal value is confirmed by using roulette strategy. According to Equation (1), each particle's location is updated. Initial temperature is determined by

$$t_0 = f(p_{gd}) / \ln(5) \tag{4}$$

where p_{gd} is the global optimal solution. The way of annealing is determined by

$$t_{k+1} = \lambda t_k \tag{5}$$

where λ is the annealing constant.

2.3. Algorithm Comparison

The Ackley's function is used to test the algorithm of basic particle swarm optimization (bPSO), modified particle swarm optimization (sPSO) and hybrid algorithm (dPSO). The convergence curve is shown in Fig. 1. The convergence precision of sPSO (II) and dPSO (III) is superior to bPSO (I). The convergence rate of dPSO is superior to bPSO and sPSO.

3. EFFECT OF DISCHARGE CIRCUIT PARAMETERS ON THE DISTRIBUTION OF THE MAGNETIC FIELD IN THE HEAD

In this paper, the charge capacitance, resistance and inductance of the coil are studied. Currently the maximum stimulation depth of the "8" coil is 2 cm, so the plane below 2 cm is taken. In this plane, the distance of Z axis direction 0 mm $\sim$ 100 mm is obtained, and the magnetic field distribution in this direction is studied. The distance of X axis in the plane is taken to study the magnetic field distribution in the direction of -60 mm $\sim$ 60 mm. The influence of three parameters on the magnetic field distribution is discussed.

3.1. Model

3.1.1. Coil Model

The coil used for TMS is "8" coil made up of two circular coils. In this paper, the outside diameter, inner diameter and number of turns of the coil are 20 mm, 2 mm and 15, respectively. A geometric structure graph is shown in Fig. 2. It is placed in the top 1 mm of the head model.
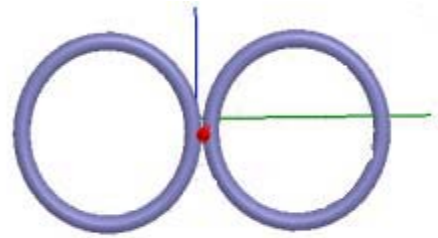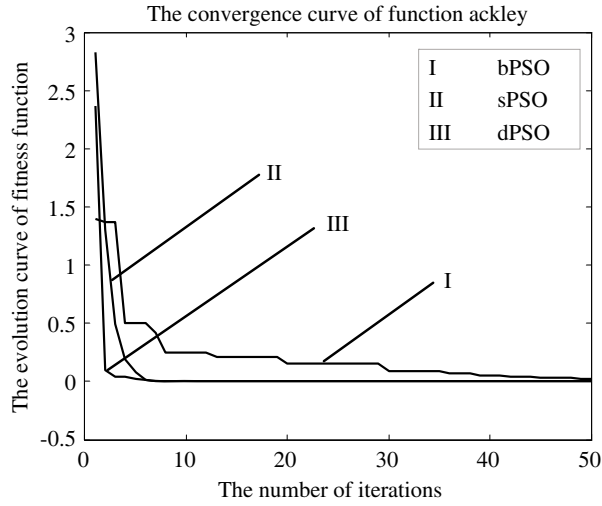
Figure 1. The convergence curve of Ackley's function.

Figure 2. Coil model.

3.1.2. Head Model

As shown in Fig. 3, the head model uses concentric spheres. The concentric sphere from the inside to the outside in order is the brain, cerebrospinal fluid, skull, scalp, and the radii are 84 mm, 86 mm, 94 mm and 100 mm, respectively. The model is located in a three-dimensional coordinate axis, and the center is the origin of the coordinates.

Different parts of biological tissues have different permeabilities, conductivities and dielectric constants. Through finding the relevant literature, the brain model of each part of the parameters is set as shown in Table 1.
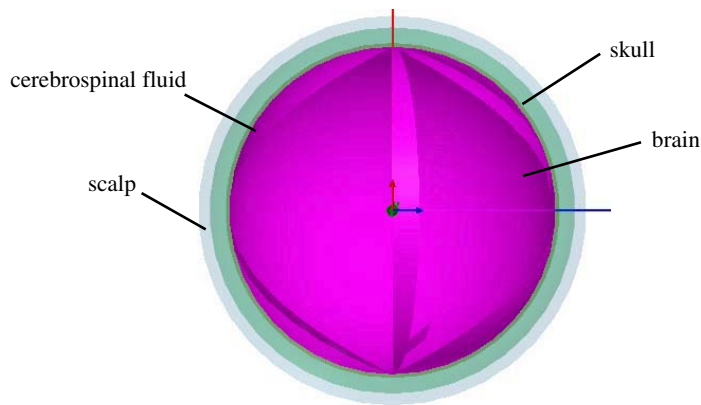

Figure 3. Geometry structure of four layer sphere head model.

Table 1. Head model organization parameters.

Head tissue	scalp	skull	cerebrospinal fluid	brain
permeability (H/m)	1	1	1	1
conductivity (S/m)	0.33	0.042	1	0.33

3.2. Simulation of the Distribution of the Magnetic Field under Different Discharge Circuit Parameters

We use a simulation software to calculate inductance of the coil. In the practical application, inductance of the coil changes with the variety of current frequencies. The influence of the current frequency is ignored in this paper. So the solver type chooses the static magnetic field. The calculated inductance value is $5.42\,\mu\mathrm{H}$. In order to study the influence of different inductance values, the inductance of the discharge circuit uses different values. This inductance will only affect the characteristics of the pulse current of the RLC oscillating circuit and will not affect the focusing of the stimulus.

When $U = 1000\,\mathrm{V}$, and different values are taken for R, L and C, the magnetic field distribution maps of $-60\,\mathrm{mm} \sim 60\,\mathrm{mm}$ in the x axis and $0\,\mathrm{mm} \sim 100\,\mathrm{mm}$ in the z axis of the $2\,\mathrm{cm}$ plane are shown in Fig. 4, Fig. 5 and Fig. 6.

It can be seen from Fig. 4, Fig. 5 and Fig. 6 that the attenuation of the magnetic field from the scalp to the brain is exponential, and the magnetic field peak value is also decreased. When L, C and R values are increased, the magnetic field values at the same position are also increased, and at the same time, the depth of the stimulus is gradually reduced.
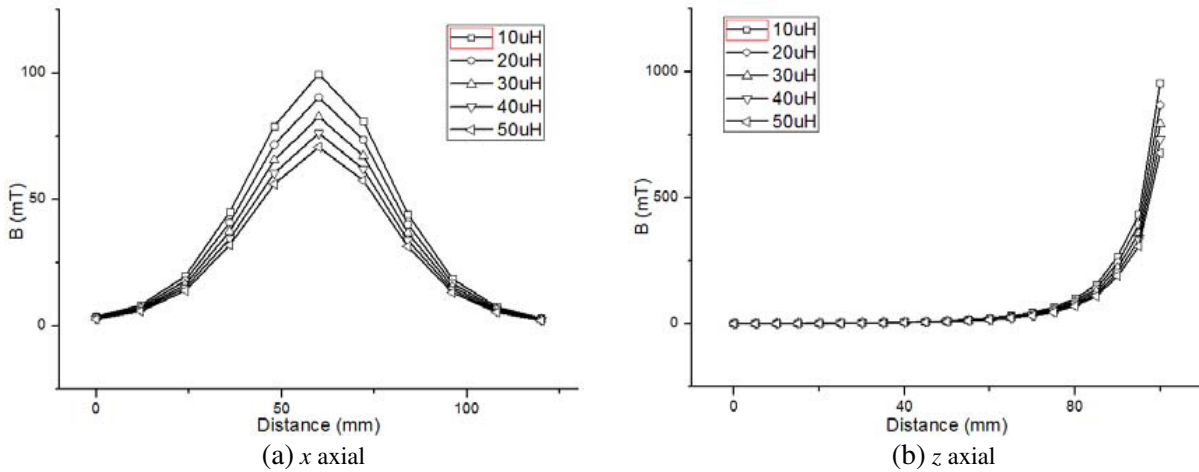

(a) x axial   (b) z axial

Figure 4. Magnetic field distribution of (a) x axial and (b) z axial with different inductance value ($C = 150\,\mu\mathrm{F}$, $R = 0.1\,\Omega$).

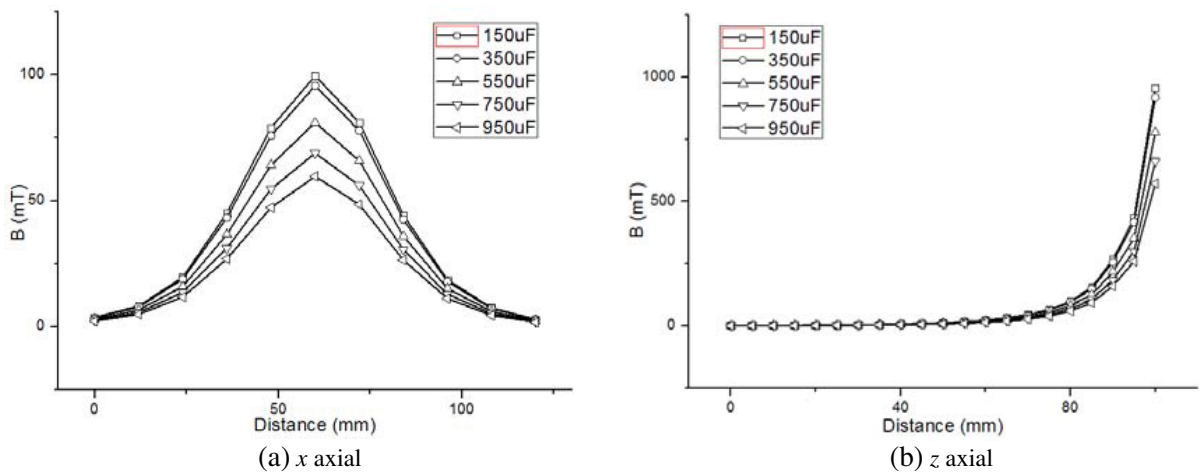(a) x axial   (b) z axial

Figure 5. Magnetic field distribution of (a) x axial and (b) z axial with different capacitance value ($L = 10\,\mu\mathrm{H}$, $R = 0.1\,\Omega$).

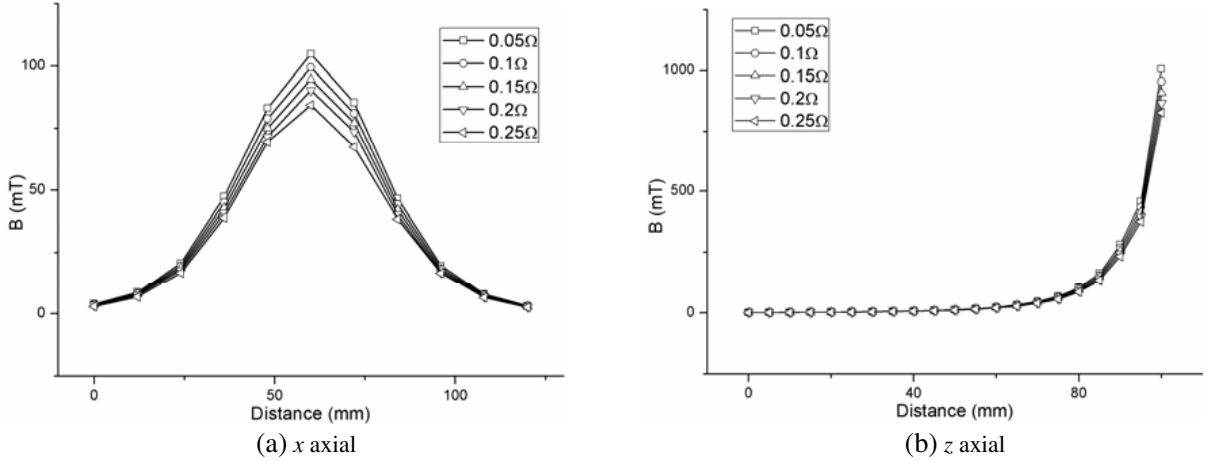(a) *x* axial   (b) *z* axial

Figure 6. Magnetic field distribution of (a) x axial and (b) z axial with different resistance value ($C = 150\,\mu\text{F}$, $L = 10\,\mu\text{H}$).

From those results, we can know that changing the *value* of L, C and R will have a big impact on the magnetic field intensity and stimulation depth. The influence of C value is more than L value, and R value is less than L and C values. Decreasing L value and increasing C and R values can effectively increase the magnetic field peak value. But as the capacitor value decreases, the pulse current peak and duration time decrease.

In conclusion, on one hand, the values of capacitance, resistance and inductance are good in some aspect, but inevitably result in decreased performance on the other hand at the same time. According to different applications and different diseases, we need to choose different discharge circuit parameters. Different disease locations and incidences of the same disease require different stimulation depths and duration times, so the parameters choice should be considered comprehensively. For example, children with ADHD need rTMS to function in an auxiliary motor area. The frequency is 0.5 Hz. The magnetic field intensity is $50\% \sim 80\%$; the sequence is 20 pulses each time; the sequence interval is 2 second. Chronic pain requires rTMS to give a high frequency (10 or 20 Hz) stimulation, and 1200 pulses to the patient can alleviate the condition at least. The cause of insomnia is that the brain is too excited, so the method for the treatment of insomnia is to stimulate the brain in low frequency.

4. RESULTS

The common coil configurations include circular coil, eight-figure coil, double eight-figure coil, double butterfly coil, 4-leaf-clover coil, H coil and Halo coil. The array coils are shown as Fig. 7. There are 5 coils. The radius of every coil is 5 mm. The radius of the sphere where the central coil is located is the minimum. The angle of the ambient four coils from each other is 90°. The angle is 45° between ambient four coils and xoy plane. The ambient four coils are tangent to the sphere whose radius is 20 mm. The plan of $Z = 0$ is the focusing plane. This design can develop the coil array's focusing effect caused by the vector superposition in the focusing plane.

In the application of TMS, the most commonly used coil is the "8" coil. But it will cause the non-target location to be excited; therefore, its use in clinical application is limited. The use of coil array is an effective method to realize magnetic focusing at present. This paper uses 5 array coils. This design can make full use of vector superposition on the focal plane. The coil array is shown in Fig. 7. Each coil radius is 20 mm. According to the results of the above, the sphere radius of the central coil is the smallest, and the included angle is 0°. The angle of the ambient four coils from each other is 90°, and the four coils are tangent to the surface of the scalp. The relative position between the coil and the head model is shown in Fig. 8.

Based on improved particle swarm optimization and simulated annealing algorithm, a hybrid optimization algorithm is used to optimize the current in the 5-coil array. The objective function
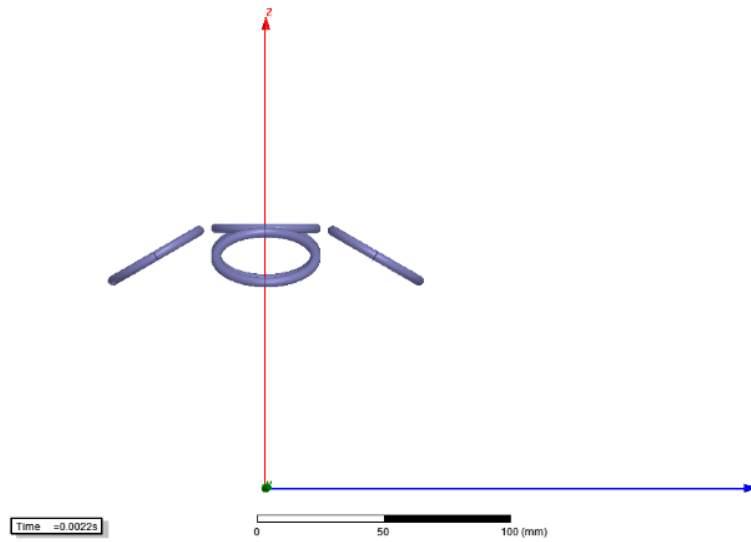
Figure 7. 5 array coils model.

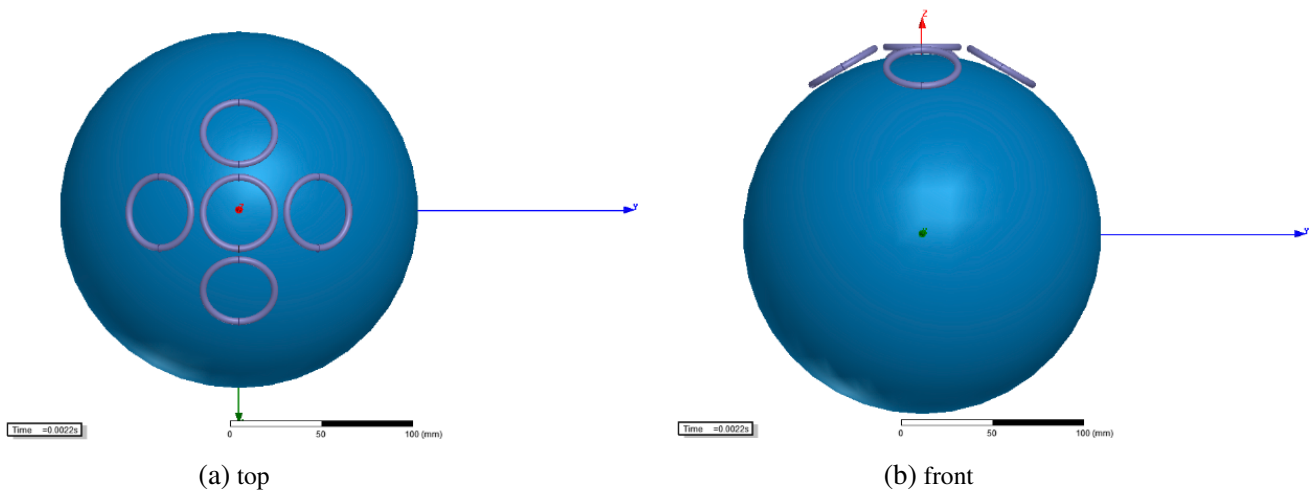(a) top   (b) front

Figure 8. The coil relative positionto (a) top view and (b) front view of the head model.

is $B_{\max}/S_{0.8}$, where $B_{\max}$ is the maximum magnetic field of the focal plane and $S_{0.8}$ the area whose magnetic field value is greater than $0.8B_{\max}$. The optimized ratio of 5-coil current is: $(-4.3:1:1:1:1)$. Adjusting the excitation voltage in the excitation circuit can change the magnitude of the coil current. The current amplitude of the center coil is $-3000\,\text{A}$ in simulation experiments, and four-coil current is about $580\,\text{A}$. Based on the study results of parameters R, L and C, those values in the excitation circuit are selected as $0.1\,\Omega$, $10\,\mu\text{H}$, $150\,\mu\text{F}$. As shown in Fig. 9(a), the magnetic field distribution is obtained under the focal plane of $2\,\text{cm}$. The magnetic field distribution curve of y axis direction on the focal plane is obtained, as shown in Fig. 10(a). To compare the effects of optimization algorithm optimization, taking the current $+3000\,\text{A}$, and R, L, C values of excitation circuit are selected $0.1\,\Omega$, $10\,\mu\text{H}$, $150\,\mu\text{F}$. The magnetic field distribution in the focal plane is shown in Fig. 9(b), and magnetic field distribution curve of y axis is shown in Fig. 10(b).

As can be seen from Fig. 9(a) and Fig. 9(b), the magnetic field value is reduced rapidly from the center to the periphery. After optimization, the distribution of the magnetic field is clearer, and the distribution of the magnetic field is concentrated in a smaller area. The area which is greater than 80% $B_{\max}$ is significantly less than the non-optimized area, and the focality is better. As can be seen from
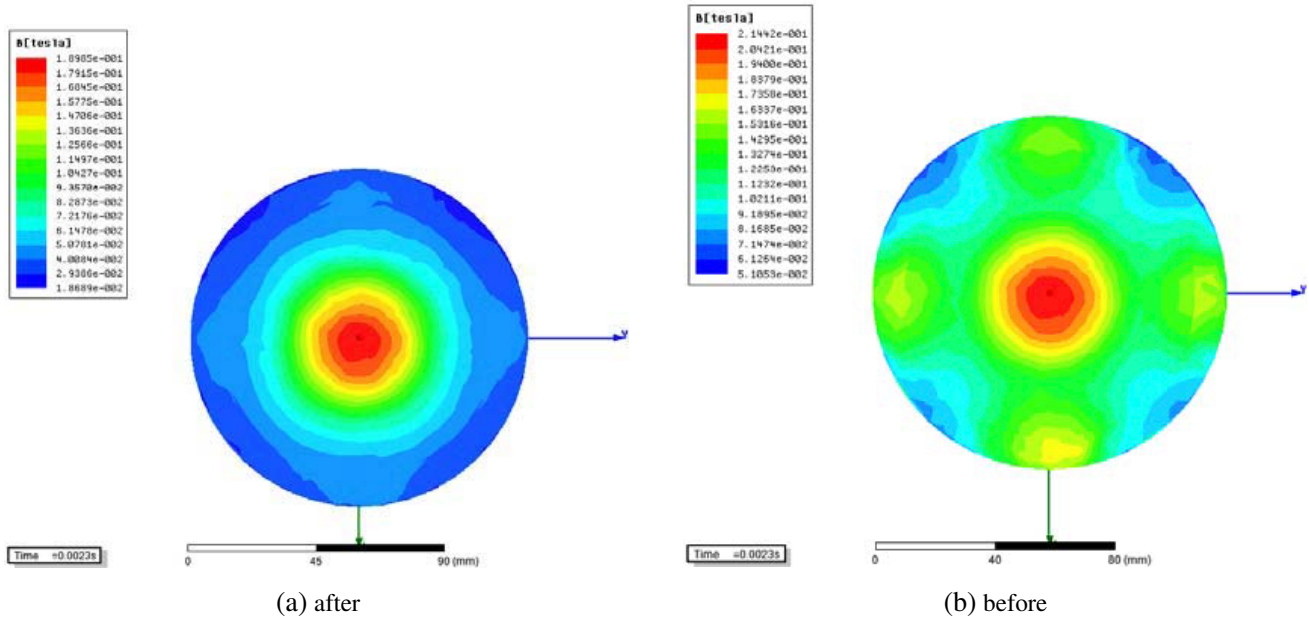
(a) after   (b) before

Figure 9. The magnetic field distribution of the focusing plane (a) after and (b) before optimization.

(a) after   (b) before
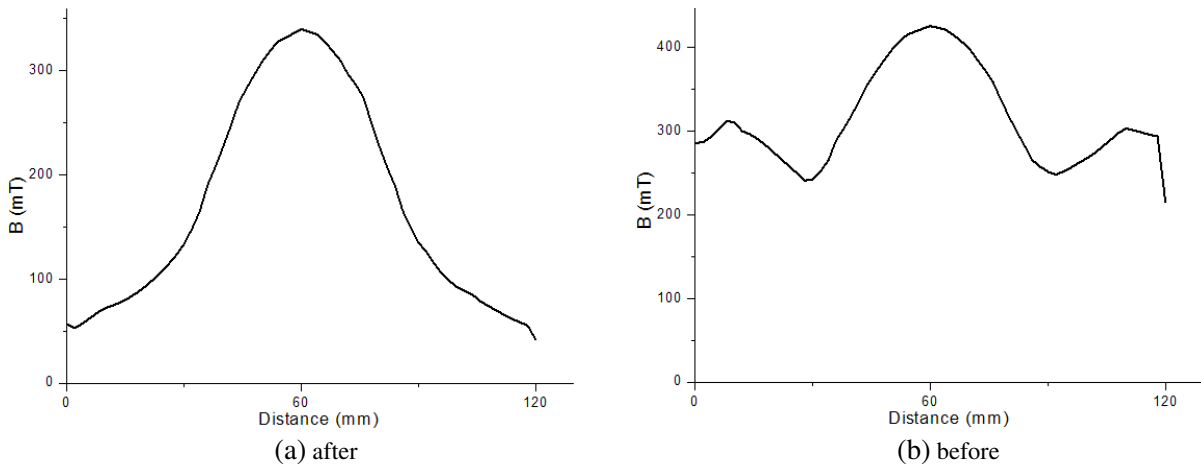
Figure 10. The magnetic field distribution of y axis (a) after and (b) before optimization.

Fig. 10(a), the magnetic field value increases at first and then decreases in the focusing plane along the Y axis. The maximum value is achieved in $y = 0$. There is only one peak and no secondary peaks, namely the magnetic field only acts on one target location. Focus waveform is steeper and more close to the sharp pulse wave. Magnetic field distribution curve is relatively flat in Fig. 10(b), and secondary peaks appear on both sides of the main peak, namely the target position and non-target position are all stimulated at the same time.

5. CONCLUSIONS

This paper studies the factors affecting the focality. A hybrid algorithm was proposed to optimize the parameters of the discharge circuit. Then, the 5 array coils were configured to achieve a comprehensive focus. From the simulation results we can have the follwing conclusions.

This hybrid algorithm which optimizes the current of the coils can achieve good focality

performance. Through the test of this hybrid algorithm, it is proved that the algorithm is short in time and has fast convergence, which is consistent with the requirement of the algorithm.

Different discharge circuit parameters are selected according to different applications and different diseases. Different locations or different levels of disease need different stimulation depths and durations of stimulation. So the parameter selection should be considered synthetically.

In the future, we will optimize other coil parameters, conduct the experiment of magnetic field and electric field distribution on the head model, and do further research on the design of the coil model. In addition, compared with electroshock therapy (ECT), TMS stimulus intensity is less than the former [21], so we will give more attention to the vertical direction and design the new coil structure to achieve depth focus. The combination of the stimulus depth and focus will be considered together to measure the effect of stimulus. We will establish a precise brain model and use the theory of electromagnetic field to accurately analyze the electromagnetic field to achieve the precise focus.

REFERENCES

1. Barker, A. T., R. Jalinous, et al., "Non-invasive magnetic stimulation of human motor cortex," *The Lancet*, Vol. 1, 1106–1107, 1985.

2. Zyss, T., A. Krawczyk, et al., "Transcranial magnetic stimulation TMS verus electroconvulsive therapy ECT in therapy of depressions — Advantages and disadvantages of computer modeling," De Gruyter, Vol. 6, No. 12, 67–73, 2010.

3. Ai, Q., J. Li, et al., "A new transcranial magnetic stimulation coil design to improve the focality," *2010 3rd International Conference on Biomedical Engineering and Informatics*, Vol. 4, 1391–1395, 2010.

4. Deng, Z. D., S. H. Lisanby, et al., "Electric field depth-focality tradeoff in transcranial magnetic stimulation: Simulation comparison of 50 coil designs," *Brain Stimulation*, Vol. 6, 1–13, 2013.

5. Laakso, I. and A. Hirata, "Fast multigrid-based computation of the induced electric field for transcranial magnetic stimulation," *Physics in Medicine & Biology*, Vol. 57, 7753–7765, 2012.

6. Okada, A., A. Nishikawa, et al., "Magnetic navigation system for home use of repetitive transcranial magnetic stimulation (rTMS)," *2012 ICME International Conference on Complex Medical Engineering (CME)*, 112–118, 2012.

7. Yang, S., G. Xu, L. Wang, and Q. Yang, "Analysis of double eight-figure coil for transcranial magnetic stimulation based on realistic head model," *2012 Sixth International Conference on Electromagnetic Field Problems and Applications*, 1–4, 2012.

8. Yang, S., G. Xu, et al., "Circular coil array model for transcranial magnetic stimulation," *IEEE Transactions on Applied Superconductivity*, Vol. 20, 829–833, 2010.

9. Li, J., Z. Liang, et al., "Double butterfly coil for transcranial magnetic stimulation aiming at improving focality," *IEEE Transactions on Magnetics*, Vol. 48, 3509–3512, 2012.

10. Zhang, S., Y. Tao, et al., "Experimental study to improve the focalization of a figure-eight coil of rTMS by using a highly conductive and highly permeable medium," *IEEE Transactions on Neural Systems & Rehabilitation Engineering*, Vol. 21, 364–369, 2013.

11. Gomez, L., F. Cajko, et al., "Numerical analysis and design of single-source multicoil TMS for deep and focused brain stimulation," *IEEE Transactions on Bio-medical Engineering*, Vol. 60, 2771–2782, 2013.

12. Lu, M. and S. Ueno, "Toward deep transcranial magnetic stimulation," *2014 XXXIth URSI General Assembly and Scientific Symposium (URSI GASS)*, 1–4, 2014.

13. Laudani, A., F. R. Fulginei, et al., "TMS array coils optimization by means of CFSO," *IEEE Transactions on Magnetics*, Vol. 51, 1–4, 2015.

14. Tachas, N. J., K. G. Efthimiadis, et al., "The effect of coil modeling on the predicted induced electric field distribution during TMS," *IEEE Transactions on Magnetics*, Vol. 49, 1096–1100, 2013.

15. Gomez, L., F. Cajko, et al., "Numerical analysis and design of single-source multicoil TMS for deep and focused brain stimulation," *IEEE Transactions on Bio-medical Engineering*, Vol. 60, 2771–2782, 2013.

16. Yang, S., G. Xu, et al., "Circular coil array model for transcranial magnetic stimulation," *IEEE Transactions on Applied Superconductivity*, Vol. 20, 829–833, 2010.

17. Clerc, M. and J. Kennedy, "The particle swarm — Explosion, stability, and convergence in a multidimensional complex space," *IEEE Transactions on Evolutionary Computation*, Vol. 6, 58–73, 2002.

18. Holden, N. and A. A. Freitas, "A hybrid particle swarm/ant colony algorithm for the classification of hierarchical biological data," *Proceedings 2005 IEEE Swarm Intelligence Symposium, 2005, SIS 2005*, 100–107, 2005.

19. Wang, H. and Z.-S. Li, "A simpler and more effective particle swarm optimization algorithm," *Journal of Software*, Vol. 18, 861–868, 2007.

20. Yu, L.-L. and Z. X. Cai, "Multiple optimization strategies for improving hybrid discrete particle swarm," *Journal of Central South University*, 2009.

21. Zyss, T., A. Krawczyk, et al., "Electroshock therapy (ECT) versus transcranial magnetic stimulation (TMS): Modeling of current flow in 3-D head structure," *European Neuropsychopharmacology*, Vol. 8, S317, 1998.